



HAL
open science

Capacity of a Bayesian model to detect infected herds using disease dynamics and risk factor information from surveillance programmes: A simulation study

M. Mercat, A.M. van Roon, I. Santman-Berends, G. van Schaik, M. Nielen, D. Graham, S.J. More, M. Guelbenzu-Gonzalo, C. Fourichon, A. Madouasse

► To cite this version:

M. Mercat, A.M. van Roon, I. Santman-Berends, G. van Schaik, M. Nielen, et al.. Capacity of a Bayesian model to detect infected herds using disease dynamics and risk factor information from surveillance programmes: A simulation study. Preventive Veterinary Medicine, 2022, 200, pp.105582. 10.1016/j.prevetmed.2022.105582 . hal-03559742

HAL Id: hal-03559742

<https://hal.inrae.fr/hal-03559742v1>

Submitted on 22 Jul 2024

HAL is a multi-disciplinary open access archive for the deposit and dissemination of scientific research documents, whether they are published or not. The documents may come from teaching and research institutions in France or abroad, or from public or private research centers.

L'archive ouverte pluridisciplinaire **HAL**, est destinée au dépôt et à la diffusion de documents scientifiques de niveau recherche, publiés ou non, émanant des établissements d'enseignement et de recherche français ou étrangers, des laboratoires publics ou privés.



Distributed under a Creative Commons Attribution - NonCommercial 4.0 International License

Capacity of a Bayesian model to detect infected herds using disease dynamics and risk factor information from surveillance programmes: A simulation study

1 M. Mercat¹, A.M. van Roon², I. Santman-Berends^{2,3}, G. van Schaik^{2,3}, M. Nielen², D. Graham⁴,

2 S.J. More⁵, M. Guelbenzu-Gonzalo⁴, C. Fourichon¹, A. Madouasse¹

3 ¹INRAE, Oniris, BIOEPAR, Nantes 44300, France

4 ²Department of Farm Animal Health, Faculty of Veterinary Medicine, Utrecht University, PO Box
5 80151, 3508, TD Utrecht, the Netherlands

6 ³Royal GD, PO Box 9, 7400 AA, Deventer, the Netherlands

7 ⁴Animal Health Ireland, Unit 4/5, The Archways, Bridge St., Carrick-on-Shannon, Co. Leitrim N41
8 WN27, Ireland

9 ⁵Centre for Veterinary Epidemiology and Risk Analysis, UCD School of Veterinary Medicine,
10 University College Dublin, Belfield, Dublin D04 W6F6, Ireland

11 * **Correspondence:**

12 Aurélien Madouasse

13 aurelien.madouasse@oniris-nantes.fr

14 **Keywords: output-based surveillance, Hidden Markov Model, herd-level probability of**
15 **infection, freedom from infection, longitudinal data, repeated testing.**

16

17 **1 Abstract-**

18 Control programmes against non-regulated infectious diseases of farm animals are widely
19 implemented. Different control programmes have different definitions of “freedom from infection”
20 which can lead to difficulties when trading animals between countries. When a disease is still present,
21 in order to identify herds that are safe to trade with, estimating herd-level probabilities of being
22 infected when classified “free from infection” using field data is of major interest. Our objective was
23 to evaluate the capacity of a Bayesian Hidden Markov Model, which computes a herd-level
24 probability of being infected, to detect infected herds compared to using test results only. Herd-level
25 risk factors, infection dynamics and associated test results were simulated in a population of herds,
26 for a wide range of realistic infection contexts and test characteristics. The model was used to predict
27 the infection status of each herd from longitudinal data: a simulated risk factor and a simulated test
28 result. Two different indexes were used to categorize herds from the probability of being infected
29 into a herd predicted status. The model predictive performances were evaluated using the simulated
30 herd status as the gold standard. The model detected more infected herds than a single final test in
31 85% of the scenarios which converged. The proportion of infected herds additionally detected by the
32 model, compared to test results alone, varied depending on the context. It was higher in a context of a
33 low herd test sensitivity. On average, around 20%, for high test sensitivity scenarios, and 40%, for
34 low test sensitivity scenarios, of infected herds that were undetected by the test were accurately
35 classified as infected by the model. Model convergence did not occur for 39% of the scenarios,
36 mainly in association with low herd test sensitivity. Detection of additional newly infected herds was
37 always associated with an increased number of false positive herds (except for one scenario). The
38 number of false positive herds was lower for scenarios with low herd test sensitivity and moderate to
39 high incidence and prevalence. These results highlight the benefit of the model, in particular for

40 control programmes with infection present at an endemic level in a population and reliance on test(s)
41 of low sensitivity.

42 **2 Introduction**

43 Various control programmes (CPs) against infectious diseases of farm animals are implemented in
44 Europe. In order to control or eradicate these diseases, CPs typically focus on the identification of
45 infected units (animals or herds) using diagnostic tests performed at regular time intervals. CPs may
46 be deployed across a territory, from regional to national scale. Testing schemes can vary in terms of
47 type and performance of the test used, the cohorts and numbers of animals tested, and the time
48 interval between tests. These differences have been documented for some endemic cattle diseases,
49 including infections by bovine viral diarrhoea virus (van Roon et al., 2020b), *Mycobacterium avium*
50 subspecies *paratuberculosis* (Whittington et al., 2019), and bovine herpesvirus 1 (Raaperi et al.,
51 2014).

52 Heterogeneity in CPs may lead to difficulties when trading animals between different regions or
53 countries, as each CP has its own definition of “freedom from infection” which cannot be directly
54 compared. These definitions of a “free status” are usually based on one, or a combination of several,
55 diagnostic test result(s). Limitations in test performance, and time interval between tests lead to
56 uncertainty around these statuses. Imperfections in the testing schemes lead to two types of error.
57 Firstly, a lack of specificity means that some uninfected herds are wrongly categorized as infected,
58 i.e. false positives. Secondly, a lack of sensitivity leads to some infected herds being wrongly
59 categorized as free from infection, i.e. false negatives. The time interval between tests may result in
60 a delay between the times of infection and detection. For herds classified as “free from infection”,
61 those that become infected between two consecutive tests will remain classified as “free from
62 infection” until a next test event. Hence, as each CP has its own surveillance strategy, the confidence

63 and associated uncertainty in the true status of a herd classified as “free from infection” may vary
64 depending on the CP. Currently when purchasing an animal from a herd classified as “free from
65 infection” under different CPs, it is not possible to assess the probability of infection for that animal.
66 As trade can be an opportunity for infectious diseases to spread, confidence in “free status” is a key
67 point to support international trade.

68 There is a need for the development of methods that enable a CP-level comparison of confidence of
69 herd-level “freedom from infection”. The traditional solution to obtain a comparable surveillance
70 output in different regions or countries is to use input-based surveillance. This type of surveillance
71 consists in prescribing how surveillance should be performed in terms sampling design, sample size
72 and tests used. However, input-based surveillance does not take into account the diversity of contexts
73 in which CPs are applied (van Roon et al., 2020b) and can be expensive to run, while not being
74 adapted to the specific context of each CP (Cameron, 2012). Alternatively, output-based surveillance
75 may be used, which is not prescriptive in terms of the elements of the programme, but rather in the
76 degree of confidence associated with a free status that must be achieved.

77 Imperfect testing regimes lead to misclassification errors, as highlighted above. To account for this,
78 known risk factors (RFs) for the introduction of infection could be included in the calculation of
79 probability of freedom, as predictors of either current or new infection. Data on such disease-specific
80 RFs should be available for many CPs, given that action on these RFs is used as a way to prevent the
81 introduction of infection. Disease-specific RFs for introduction depend on the pathogen as well as the
82 route of transmission (direct or indirect transmission). For many diseases, animal purchase is a
83 common RF for introduction of infection into herds (Rangel et al., 2015; van Roon et al., 2020a). In
84 the European Union, where cattle identification and the recording of cattle movements between
85 holdings are mandatory, these data could be used to predict (new) infections through purchase, thus
86 contributing to improved estimation of the infection-free status of a herd.

87 In Madouasse et al. (2021), a modelling framework was described, called the STOC free
88 (Surveillance analysis Tool for Output based Comparison of the confidence of FREEdom from
89 infection) model, that estimates the herd-level probabilities of infection, using data from CP and
90 taking RF occurrence into account. The model estimates the probability of infection at the last time-
91 step for each herd (in a series of sequential test results). Model inputs include repeated test results
92 and the presence of RFs for each herd as measured regularly within the surveillance programme. The
93 framework incorporates knowledge at the population level on infection dynamics, test characteristics
94 and the effect of RFs when estimating probability of infection.

95 In order to evaluate the capacity of the STOC free model to detect infected herds, a gold standard is
96 required. Gold standard is the true herd status. In the context of the STOC free model, an infected
97 herd is defined as the presence of at least one infected animal. To measure the true status of the herd,
98 it would be necessary to test all the animals within a herd using a perfect test. However, no such data
99 exist in the real-world. Up to now, the STOC free model has only been applied to a single French
100 dataset, which included test results and RFs but no gold standard (Madouasse et al., 2020). An
101 evaluation of the performance of this model under different circumstances is therefore lacking.

102 The use of simulated data is an effective way to evaluate the predictive accuracy of the STOC free
103 model given the absence of gold standard information in real-world surveillance data. This approach
104 has been used for the evaluation of latent-class models for the estimation of infection prevalence in
105 dairy herds (McAloon et al., 2019). Data simulation allows a simplified system to be created where
106 the true herd status is known. Simulated surveillance data, i.e. test results and RF information
107 collected at regular intervals, can be used as input for the STOC free model as an alternative to real-
108 world surveillance data. The performance of the model can be then evaluated by looking at errors in
109 herd status classification, by comparing true herd status to the status predicted by the model.

110 Furthermore, compared to real data, using simulated data enables a wide range of epidemiological

111 situations and surveillance modalities to be evaluated. It makes it possible to investigate the potential
112 of the model to be used for different diseases where performance of CPs differs.

113 The objective of this work was to evaluate the capacity of the STOC free model, which takes account
114 of both dynamics of testing and risk factor information, to improve the detection of infected and
115 newly infected herds compared to test results alone (i.e. the added value of the model in sensitivity).
116 Among infected herds, newly infected are the ones which were not infected at the previous test event.
117 We assumed that the added value of the model in terms of the detection of newly and previously
118 infected herds could be different depending on the epidemiological context (impact of relative risk
119 associated and frequency of risk factor and disease dynamics) and test performances (sensitivity and
120 specificity). Simulated data were used to generate a wide range of realistic CPs (different CP
121 corresponding either to different diseases or to the results of different testing strategies for a disease
122 in different contexts). We quantified the number of additional infected herds detected by the STOC
123 free model compared to test results.

124 **3 Material and methods**

125 **3.1 Overall design strategy**

126 Firstly, a dynamic model was developed to simulate herd-level infection and surveillance data under
127 a wide variety of CP scenarios corresponding either to different diseases or to the results of different
128 testing strategies for a disease in different contexts. The simulated surveillance data were then used
129 as input for the STOC free Bayesian Hidden Markov Model, which was run to generate outputs on
130 model parameters estimates and predicted herd status for probability of infection at the last time-step.
131 Finally, model and test performance were compared. The overall design strategy is presented in
132 Figure 1.

133 **3.2 Simulation of herd infection and surveillance data model**

134 We simulated the dynamics of herd infection status depending on the presence of a single RF
135 associated with an increased probability of becoming infected, generating data on herd status and test
136 results at each time-step. Initially, RF presence/absence was simulated. Herd infection status at the
137 first time-step was based on the chosen simulated prevalence of infection. Then, at a given time-step,
138 non-infected herds could become infected according to a probability of new infection between time-
139 steps, which varied depending on RF occurrence. The probability that an infected herd would remain
140 infected between two sequential time-steps was determined by a simulation parameter that
141 represented this probability (of infection not being resolved between two different time-steps).
142 Infection status for a given herd at a given time-step determined the result of a test, assuming a given
143 herd-level test sensitivity and specificity.

144 **3.2.1 Simulation of herd status at each time-step**

145 Infection dynamics were simulated by herd status change. Herd status was simulated as a binary
146 event, with 0 and 1 denoting absence and presence of infection, respectively. Herd status was
147 assumed to undergo Markovian dynamics with status at time t depending on status at time $t-1$ and RF
148 occurrence. In each scenario, the overall herd infection prevalence was held constant over the time-
149 steps to evaluate the STOC free model in different situations over a short period. Keeping the
150 prevalence constant prevents the infection of either dying out or rapidly increasing over the number
151 of time-steps and allows a comparable number of infected herds to be detected. For consistency, the
152 probability of new infection between time-steps was a function of both overall herd infection
153 prevalence and the probability of a herd remaining infected between time-steps to allow overall
154 prevalence to remain constant over time.

155 Status simulation can be described by the following set of equations. In herd h at time t , the infection
156 status $S_{h,t}$, was sampled from a Bernoulli distribution:

157
$$S_{h,t} \sim \text{Bernoulli}(\pi_{h,t}) ,$$

158 with $\pi_{h,t}$ being the probability of being infected at time-step t for herd h . For a given herd at time
159 $t=1$, the probability of infection was:

160
$$\pi_{h,t=1} = P ,$$

161 with P being the herd infection prevalence for that scenario. For a given herd h at time $t > 1$, $\pi_{h,t}$
162 depended on previous status and infection dynamics parameters:

163
$$\pi_{h,t} = (1 - S_{h,t-1})\tau_1^{h,t} + S_{h,t-1}\tau_2 ,$$

164 with $S_{h,t-1}$ being the status of herd h at the previous time-step, τ_2 being the probability of remaining
165 infected between time-steps (fixed variable in each scenario), and $\tau_1^{h,t}$ the probability of new
166 infection between time-steps which was defined as a function of herd-level risk factor exposure and
167 defined as:

168
$$\tau_1^{h,t} = (1 - X_{h,t-1})\beta + X_{h,t-1}\beta\gamma ,$$

169 where β was the probability of new infection when the risk factor was absent, i.e. $X_{h,t-1} = 0$ and $\beta\gamma$
170 was the probability of new infection when the RF was present, i.e. $X_{h,t-1} = 1$. Thus, γ was the
171 relative risk of new infection in herds exposed to the RF. Exposure to the RF (X) was considered a
172 random dichotomous variable simulated as:

173
$$X_{h,t} \sim \text{Bernoulli}(F) ,$$

174 with F being the RF frequency in the data set.

175 Assuming an endemic situation with a constant prevalence over time-steps, at each time-step in each
176 scenario the average number of newly infected herds was constrained to be equal to the average
177 number of herds eliminating the infection. Therefore, the following condition had to be met:

$$178 \quad E(\tau_1^{h,t})(1 - P) = (1 - \tau_2)P ,$$

179 where $E(\tau_1^{h,t})$ was the expectation for the probability of new infection. This amounts to applying the
180 following constraint on the overall probability of new infection:

$$181 \quad E(\tau_1^{h,t}) = \frac{(1-\tau_2)P}{1-P} .$$

182 From the definition of $\tau_1^{h,t}$ and the frequency of the RF, F , at a given time-step, the expected
183 probability of new infection was:

$$184 \quad E(\tau_1^{h,t}) = (1 - F)\beta + F\beta\gamma ,$$

185 where γ was the relative risk of new infection in herds exposed to the RF and β the probability of
186 new infection in herds that were not exposed to the RF. The frequency of the RF (F) and the relative
187 risk of new infection in herds exposed to the RF (γ) are inputs in the simulation. The probability of
188 new infection in herds that were not exposed to the RF (β) can be computed as:

$$189 \quad \beta = \frac{E(\tau_1^{h,t})}{1+F(\gamma-1)} .$$

190 3.2.2 Simulation of test results

191 A test result was simulated for each herd at each time-step as a function of the simulated herd status,
192 the herd-level test sensitivity and specificity. Test result in herd h at time t was sampled from a
193 Bernoulli distribution:

$$194 \quad T_{h,t} \sim \text{Bernoulli}(p(T_{h,t}^+)) ,$$

195 with $p(T_{h,t}^+)$ being the probability of being tested positive defined by:

$$196 \quad p(T_{h,t}^+) = S_{h,t}Se + (1 - S_{h,t})(1 - Sp) ,$$

197 with Se and Sp being respectively herd-level test sensitivity (probability for an infected herd to be
198 tested positive) and specificity (probability for an uninfected herd to be tested negative).

199 3.3 Input scenario: differing infection and epidemiological situation

200 We simulated various scenarios to represent different diseases in different contexts and different tests
201 performances for which STOC free model could be used. Different range of values for the 10
202 different parameters of the data simulation are presented in Table 1. For all scenarios, the number of
203 simulated herds was set at 5,000 and the number of simulated time-steps to 6. At each time-step, test
204 results and RF information were available. The choice of parameter values was based on knowledge
205 and discussion with a group of infectious disease experts, from different countries involved in the
206 STOC free consortium, to represent variation in context for different endemic situations.

207 Various epidemiological situations were simulated to represent various endemic infections and
208 contexts. We simulated two prevalence values, 0.3 and 0.1, representing territories in the beginning
209 of their CP and territories already in an advanced stage of control, respectively. The probability of
210 remaining infected depends on the effectiveness of herd-level eradication measures in the CP. We

211 consider high values, from 0.75 to 0.9, consistent with endemic infection dynamics. For consistency
212 with a constant prevalence of infection, the probability of becoming infected (τ_1) was calculated for
213 all combinations of P and τ_2 values (4 values).

214 Various effect of RFs on infection dynamics have been simulated to account for variability between
215 CP. We simulated low to high RF frequency setting a maximum frequency of 0.5 considering that a
216 more frequent risk factor would not be discriminatory between herds. In contrast, we have set a
217 minimum frequency at 0.1 because a very rare RF (below 0.1) will only bring information for a small
218 number of herds. The relative risk of new infection in herds exposed to the RF (γ) ranged from 1.5 to
219 5, given that RF association may be variable depending on the infection and territory (van Roon et
220 al., 2020a).

221 The test sensitivities and specificities considered in this paper measure test performance for the
222 detection of infection at the herd-level. These parameters depend on test characteristics at the animal
223 level, the number of animals tested and within-herd prevalence (Christensen and Gardner, 2000).
224 Therefore, herd-level sensitivity and specificity can differ from specific test characteristics and
225 context (Duncan and Humphry, 2016; Nielsen and Toft, 2008). We simulated herd-level sensitivity
226 from 0.4 to 0.9 and herd-level specificity from 0.8 to 0.95. Low herd-level sensitivity values
227 represent infections for which highly sensitive tests are not available, e.g. paratuberculosis (Nielsen
228 and Toft, 2008). We considered a sensitivity of 0.9 as the maximum value. In case of higher
229 sensitivity, we hypothesized that there would be limited added value from the STOC free model.
230 After taking into account the complete testing process, which often includes retesting of positive
231 herds, high values of specificity were considered appropriate. Low diagnostic specificity is less
232 common in CPs.

233 Combinations of parameters values represented the simulation of 216 different scenarios. Simulation
234 of herd infection and surveillance data model were implemented in R software (R Core Team, 2017).

235 **3.4 Description and use of the STOC free model**

236 The model described by Madouasse et al., 2020, represents infection presence at herd level as a
237 latent status over time-steps. The latent status is evaluated at regular time intervals through testing.
238 Tests may be imperfect, i.e. with a sensitivity and a specificity less than 1. The variable of interest
239 (the latent status) has a Markovian dynamic: the latent status at a given time-step depends on both the
240 latent status at the previous time-step and actions taken or RF occurrence since the previous time-
241 step. Risk factors are incorporated as predictors for new infection. The model predicts the probability
242 of infection in the final time-step for each herd in the CP. Data collected before the final time-step are
243 used as historical data for the estimation of the different model parameters, including previous latent
244 statuses. Parameters estimation and prediction are performed in a Bayesian framework.

245 **3.4.1 Model Structure**

246 To describe the STOC free model and explain how predictions were performed, we use the following
247 notation: $\hat{\beta}$ is the estimated value of β and \tilde{y} is the predicted value of y .

248 **Latent state.** We consider two latent states: 0 for uninfected herds and 1 for infected herds. For a
249 given herd h at a given time t , status $\hat{S}_{h,t}$ follows a Bernoulli distribution:

$$250 \quad \hat{S}_{h,t} \sim \text{Bernoulli}(\hat{\pi}_{h,t}),$$

251 with $\hat{\pi}_{h,t}$ being the probability of being infected. At $t=1$, a beta prior is used for $\hat{\pi}_{h,t=1}$, representing
252 initial prevalence:

$$253 \quad \hat{\pi}_{h,t=1} \sim \text{Beta}(\alpha_{\pi}, \beta_{\pi}).$$

254 **Infection dynamics.** From the second time-step on, the probability of being infected at t depends on
 255 the latent state at $t - 1$. Herds that were uninfected at $t - 1$ (i.e. $\hat{S}_{h,(t-1)} = 0$) can become infected
 256 with probability of new infection $\hat{\tau}_1^{h,t}$. Infected herds remain infected with a probability of remaining
 257 infected $\hat{\tau}_2$:

$$258 \quad \hat{\pi}_{h,t} = (1 - \hat{S}_{h,(t-1)})\hat{\tau}_1^{h,t} + \hat{S}_{h,(t-1)}\hat{\tau}_2 .$$

259 A beta prior is used for the probability of remaining infected, which is constant over time and herds:

$$260 \quad \hat{\tau}_2 \sim \text{Beta}(\alpha_{\tau_2}, \beta_{\tau_2}).$$

261 **Probability of new infection.** The probability of new infection $\tau_{i,t}^1$ is modelled as a function of the
 262 presence or absence of the RF $X_{h,t-1}$ using a logistic regression:

$$263 \quad \text{logit}(\hat{\tau}_1^{h,t}) = \hat{\theta}_1 + \hat{\theta}_2 X_{h,t-1} .$$

264 Normal priors are used for logistic regression parameters $(\hat{\theta}_1, \hat{\theta}_2)$:

$$265 \quad \hat{\theta}_1 \sim \text{Normal}(\mu_1, \sigma_1) ,$$

$$266 \quad \hat{\theta}_2 \sim \text{Normal}(\mu_2, \sigma_2).$$

267 **Test results.** Test results are considered as an imperfect measure of the latent status. We consider
 268 two herd-level test results: positive or negative (discrete). Each result follows a Bernoulli distribution
 269 with a probability $p(T^+)_{h,t}$ of being positive:

$$270 \quad T_{h,t} \sim \text{Bernoulli}\left(p(T_{h,t}^+)\right) ,$$

271 with $p(T_{h,t}^+)$ depending on estimate latent status at t and test characteristics: herd-level sensitivity
 272 (\widehat{Se}) and specificity (\widehat{Sp}):

$$273 \quad p(T_{h,t}^+) = \widehat{Se}\widehat{S}_{h,t} + (1 - \widehat{Sp})(1 - \widehat{S}_{h,t}).$$

274 Beta priors are used for test characteristics parameters:

$$275 \quad \widehat{Se} \sim \text{Beta}(\alpha_{Se}, \beta_{Se}),$$

$$276 \quad \widehat{Sp} \sim \text{Beta}(\alpha_{Sp}, \beta_{Sp}).$$

277 **3.4.2 Predicting the probability of infection**

278 The model predicts the herd-level probability of being infected at the last time-step using status
 279 prediction from the previous month, estimated infection dynamic parameters, and estimated test
 280 specificity and sensitivity.

281 First, the model predicts the probability of being herd status positive (noted $p(\tilde{S}_{h,t}^{+*})$) depending on
 282 previous predicted status ($\hat{S}_{h,t-1}^+$) and estimated infection dynamics parameter ($\tilde{\tau}_1^{h,t}, \hat{\tau}_2$):

$$283 \quad p(\tilde{S}_{h,t}^{+*}) = p(\tilde{S}_{h,t}^{+*} | p(\hat{S}_{h,t-1}^+, \tilde{\tau}_1^{h,t}, \hat{\tau}_2)),$$

284 with

$$285 \quad \tilde{\tau}_1^{h,t} = \text{logit}^{-1}(\hat{\theta}_1 + \hat{\theta}_2 X_{h,t-1}).$$

286 Then, it combines this prediction to test results to compute the final predicted probability of being
 287 infected (noted $p(\tilde{S}_{h,t}^+)$):

$$288 \quad p(\tilde{S}_{h,t}^+ | T_{h,t}^+, \tilde{S}_{h,t}^{+*}) = T_{h,t}^+ \cdot \frac{\widehat{Se} \cdot p(\tilde{S}_{h,t-1}^+)}{\widehat{Se} \cdot p(\tilde{S}_{h,t-1}^+) + (1 - \widehat{Sp}) \cdot (1 - p(\tilde{S}_{h,t-1}^+))} + (1 - T_{h,t}^+) \cdot \frac{(1 - \widehat{Se}) \cdot p(\tilde{S}_{h,t-1}^+)}{(1 - \widehat{Se}) \cdot p(\tilde{S}_{h,t-1}^+) + \widehat{Sp} \cdot (1 - p(\tilde{S}_{h,t-1}^+))},$$

289 with $T_{h,t}^+$ being test results at final step time, and \widehat{Se} and \widehat{Sp} being test characteristics parameters
290 estimated by the model. The way to estimate these predicted probability and test results is presented
291 in supplementary materials.

292 **3.4.3 Choice of prior distribution**

293 The STOC free model requires prior distributions for six different parameters: \widehat{Se} , \widehat{Sp} , $\widehat{\tau}_2$, $\widehat{\pi}_{h,t=1}$,
294 $\widehat{\theta}_1$ and $\widehat{\theta}_2$. The distributions and distribution parameters used are summarized in Table 2. We used
295 Beta distributions for parameters bounded between 0 and 1. The Beta distribution requires two
296 parameters. The α and β parameters were estimated using the mean and variance. In our model, a
297 Beta prior was used for the probability of being infected at time-step 1 $\widehat{\pi}_{h,t=1}$, test characteristics \widehat{Se}
298 and \widehat{Sp} or the probability of remaining negative $\widehat{\tau}_2$. We used true input simulated parameter values as
299 the means. The mean value was associated with low variance to build informative priors. We
300 consider that in the case of using real data accurate information would be available to construct such
301 prior. We used a Normal prior for the logistic regression parameter ($\widehat{\theta}_1$ and $\widehat{\theta}_2$) centred on the true
302 value. Types of priors and distribution parameters used are summarized in Table 2. Example of the
303 95% credibility intervals are displayed in the supplementary material.

304 **3.5 Evaluation of STOC free model output**

305 For each scenario, the STOC free model produced different outputs. The model returns Markov
306 Chain Monte Carlo (MCMC) samples from the posterior distributions model parameters and
307 probabilities of being infected at the last time-step. Model parameters include parameters related to
308 infection dynamics, association between RF and probability of new infection and test characteristics.
309 Estimations of these model parameters are performed from historical data on test results and RFs (in
310 our case, data from the first five time-steps) as well as from the prior distributions for the different
311 model parameters. First, we evaluated the convergence of the MCMC chains as well as the

312 consistency between estimated model parameters and the parameters used for simulating the data.
313 Then, from the posterior distributions of the herd-level probabilities of infections, rules were defined
314 to categorize herds as infected or uninfected. Error rates of the STOC free model were computed and
315 compared to simulated test results to enable computation of model performance.

316 **3.5.1 Evaluation of model parameter estimation**

317 **3.5.1.1 Assessing MCMC convergence**

318 The STOC free model were implemented in the JAGS computer programme (Plummer, 2003). The
319 model was applied to each scenario, running 4 chains in parallel. We removed the first 1,000
320 iterations as burn-in. Then 5,000 more iterations were run, of which one in five iterations was stored
321 for analysis, to reduce the size of the output file. For each parameter, the posterior distribution was
322 built with 4000 iterations (1000 for each chain). We used the Gelman-Rubin statistics (\hat{r}) to assess
323 convergence of the chains (Gelman and Rubin, 1992). This statistic was computed for the five
324 parameters estimated by the model (\widehat{Se} , \widehat{Sp} , $\hat{\tau}_2$, $\hat{\theta}_1$ and $\hat{\theta}_2$). We considered that scenarios with \hat{r}
325 values less than 1.05 had converged. Scenarios that did not reach convergence using 1,000 iterations
326 of burn-in were run again using 5,000 iterations of burn-in. Scenarios that did not reach convergence
327 after this second step were excluded for the rest of the analysis. To again run these scenarios with
328 more iterations would have been too time consuming.

329 **3.5.1.2 Verification of parameter estimation**

330 Parameter estimation was verified by comparing the posterior distributions to the empirical parameter
331 values within the simulated populations. In the data simulation process the value of a parameter can
332 differ between the chosen value for simulating a scenario and the resulting simulated population
333 value. For example, because of the stochasticity in the simulations, for a chosen sensitivity of 0.7 as a
334 simulation parameter there could have been 695 simulated test positives out of 1000 simulated

335 infections. In this case, the empirical sensitivity of 0.695 was used as the reference to evaluate the
336 posterior distribution for sensitivity.

337 **3.5.2 Evaluation of model prediction performances**

338 The STOC free model returns distributions of the predicted posterior probability of being infected for
339 the 5000 herds at the last time-step (Figure 1). In order to evaluate the performance of the model for
340 the prediction of true infection status, these probability distributions were discretised into *predicted*
341 *infected* or *predicted uninfected* status. First, each herd posterior probability of being infected was
342 summarised. The median probability per herd was used as the summary value as it was the variable
343 that best discriminated between uninfected and infected herds (results not shown). Then, a cut-off
344 value was applied to the summary values to classify herds as predicted infected or uninfected. The
345 general framework of the prediction performances analysis is presented in Figure 2.

346 Two different indices were used to select the cut-off value, corresponding to two different objectives
347 and are described below. Those two methods are based on knowledge of true herd status. In our
348 study, we used the simulated herd status as the gold standard, which allowed the number of true
349 positive (TP), false positive (FP), false negative (FN), and true negative (TN) to be calculated. TP
350 herds are infected herds classified infected, FN are infected herds classified uninfected, FP are
351 uninfected herds classified infected and TN are uninfected herds classified uninfected. We computed
352 them using the STOC free model or the test, represented by corresponding subscript (e.g. TP_{STOCfree}
353 and TP_{test}).

354 **3.5.2.1 Identification of cut-off value using Youden's index**

355 Firstly, we used all herd predictions at the last time-step to estimate the cut-off value which
356 minimized classification error (i.e. false positive and false negative). The cut-off choice was

357 determined using the criterion below (Youden, 1950), noting that it is a trade-off between sensitivity
358 and specificity:

359
$$\text{Youden's index} = \max(Se + Sp) ,$$

360 with

361
$$Se = \frac{TP_{STOCfree}}{TP_{STOCfree} + FP_{STOCfree}} ,$$

362 and

363
$$Sp = \frac{TN_{STOCfree}}{TN_{STOCfree} + FN_{STOCfree}} .$$

364 We ran this analysis using pROC packages in R software.

365 We compared STOC free model performances to test performances. We firstly compared the number
366 of accurately classified herds (TN+TP) by the STOC free model and by the test. Then, we explored
367 the impact of the simulation parameter values on the additional number of infected herds (TP)
368 detected by the STOC free model compared to test results.

369 We applied this cut-off value to a sub-group of the population, specifically only herds that were not
370 infected at the step before prediction (i.e. candidate herds for new infection), using true simulated
371 herd status, to allow us to distinguish between herds remaining uninfected and newly infected herds.

372 We compared STOC free model performances to test performances by doing the same analysis as
373 described above.

374 **3.5.2.2 Alternative cut-off optimizing detection of newly infected herds**

375 We explored an alternative method to choose a cut-off value designed to evaluate the performances
376 of the model for detection of newly infected herds compared to testing. We selected herds that were

377 candidates to be newly infected. With this approach, we firstly constrained the cut-off value to detect
378 at least one more newly infected herd compare to test results:

$$379 \quad \text{Number of additional TP} = TP_{STOCfree} - TP_{test} > 0 .$$

380 For cut-off values that verified this condition, we computed the associated additional number of false
381 positive (FP):

$$382 \quad \text{Number of additional FP} = FP_{STOCfree} - FP_{test} .$$

383 Finally, we computed the NewI cost index. This index was based on a trade-off between the
384 additional numbers of true positive herds and of false positive herds in the STOC free model
385 compared to test results:

$$386 \quad \text{NewI cost index} = \frac{\text{Number of additional FP}}{\text{Number of additional TP}} .$$

387 We chose the cut-off value with the lowest value of NewI cost index. This NewI cost index
388 represents the additional number of false positive for each additional true positive detected by the
389 model compared to the test results. When the NewI cost index is negative, the STOC free model
390 classifies less herds as FP and more herds as TP compared to the test results. A NewI cost index of 1
391 implies that using the STOC free model we had one additional FP for each additional TP. When the
392 NewI cost index is positive (and more than one), there is more than one additional FP for each
393 additional TP using the STOC free model.

394 In addition, cut-off values selected with both methods (Youden index and NewI cost index) were
395 compared.

396 **4 Results**

397 **4.1 Evaluation of model parameter estimation**

398 **4.1.1.1 Assessing MCMC convergence**

399 Of the 216 scenarios, 131 had a $\hat{r} < 1.05$ for all parameters (\widehat{Se} , \widehat{Sp} , $\hat{\tau}_2$, $\hat{\theta}_1$ and $\hat{\theta}_2$) which confirmed
400 convergence. For the 85 other scenarios, at least one of the five estimated parameters had a $\hat{r} > 1.05$.
401 For most of these scenarios (71/85), θ_1 chains did not converge. There were fewer scenarios where
402 Se , Sp , τ_2 and θ_2 chains did not converge (21, 28, 43 and 37 of 85 scenarios, respectively). These
403 scenarios were re-run using a greater number of iterations during burn-in. From those 85 scenarios,
404 41 subsequently converged.

405 The proportion of scenarios that finally converged (with either 1,000 or 5,000 iterations) varied
406 between values of the simulation parameters (Figure 3). About half of the scenarios (38/72) with a
407 test sensitivity of 0.4 did not converge, and about a third of the scenarios (34/108) with a test
408 specificity of 0.8 did not converge. The values of these two simulation parameters (Se and Sp) had
409 the biggest impact on convergence (Figure 3). Considering both parameters, it appears that higher
410 specificity values helped the model to converge for lower and medium, but to a lesser extent with
411 sensitivity values of 0.4 and 0.7. However, it did not make any difference for scenarios with higher
412 sensitivity values (Figure 4).

413 **4.1.1.2 Checking parameters estimation**

414 Of the 172 scenarios for which model convergence was validated, the simulated parameter value was
415 not within the 95% credibility interval of the posterior distribution, for at least one of the simulation
416 parameters, in 13 scenarios. For each of these 13 scenarios, the parameter for which this was the case
417 varied. This corresponds to 14 parameters i.e. 1.6% of the cases (14/860) for which the true value is
418 outside the 95% credibility interval. The gap between the 95% confidence interval of the posterior

419 distribution and the simulated population value was low for each of the 14 parameters
420 (supplementary material).

421 **4.2 Evaluation of model prediction performances**

422 Performances of the model were analysed for the 172 scenarios that did converge. Table 3
423 summarizes the number of scenarios for each simulation parameter value remaining at this step.

424 **4.2.1 Ability to detect infected herds in the whole population**

425 With the cut-off based on the Youden index to select the “best” cut-off to classify the whole
426 population, the model accurately classified more infected herds in 152 of the 172 scenarios compared
427 to test results alone (Figure 5). The difference between the model and test results varied from 125
428 fewer to 509 additional infected herds detected. On average the model detected an additional 105
429 truly infected herds. This represented a proportion of infected herds additionally detected by the
430 STOC free model from -0.085 to 0.358, with a mean value of 0.110, corresponding to the added
431 value in sensitivity of the surveillance scheme provided by the model (Figure 6).

432 For all scenarios with herd test sensitivity (Se) of 0.4 and 0.7, the STOC free model detected more
433 infected herds than the test results (Figure 6). For 12 out of 34 scenarios with low sensitivity, the
434 STOC free model detected an additional 0.3 proportion of infected herds than the test, with a mean
435 value of 0.258. Conversely, when sensitivity was high (0.9) the mean value of additional proportion
436 of infected herds was 0.022. Additionally, for all but two scenario with a herd test specificity (Sp) of
437 0.95, the STOC free model detected more infected herds than the test (Figure 6). The proportion of
438 herds additionally detected was similar whatever the values of the infection dynamics parameters
439 (prevalence (P), incidence rate (τ_1), and probability to remain infected (τ_2)) and RF link parameters
440 (frequency (F) and relative associated risk (γ)) (Figure 6).

441 **4.2.2 Classification of uninfected herds**

442 With the cut-off based on the Youden index, the number of herds classified as false positives
443 increased in 126 scenarios with the model (Figure 5). Only 27 of the 172 scenarios had a higher
444 number of both infected and uninfected herds that were accurately classified. They were mainly
445 associated with medium and high values of sensitivity (0.7, 0.9), the lowest value of specificity (0.8)
446 and the highest value of probability of remaining infected (τ^2) (0.9).

447 **4.2.3 Ability to detect newly infected herds among candidates to new infection**

448 **4.2.3.1 Using Youden index**

449 With the cut-off based on the Youden index, the STOC free model accurately classified more newly
450 infected herds in 65 scenarios compared to the test results (Figure 7). The difference between the
451 model and test results varied from 82 fewer to 88 more newly infected herds detected. On average,
452 the model detected 5 fewer herds than the test. This corresponded to a proportion of newly infected
453 herds additionally detected by the STOC free model from -0.603 to 0.370, with a mean value of -
454 0.046 (Figure 8).

455 Interestingly, for all scenarios with herd test sensitivity of 0.4, the STOC free model detected more
456 newly infected herds than the test results, with the additional proportion of newly infected herds
457 detected ranging from 0.008 to 0.370 (Figure 8). For 48 of the 98 simulated scenarios with a herd test
458 specificity of 0.95, the model detected more truly newly infected herds than the test alone.

459 **4.2.3.2 Using NewI cost index**

460 We developed a new index to select cut-off values, with the constraint to detect at least one more
461 newly infected herd compared to the test. For 13 of the 172 scenarios, no cut-off value allowed the
462 detection of at least one additional newly infected herd. For all the 159 remaining scenarios, using
463 this index allowed the detection of an additional proportion of newly infected herds, ranging from

464 0.003 to 0.429, with a mean value of 0.071 (Figure 9). This corresponded to the detection of 1 to 156
465 additional newly infected herds with a mean value of 14 herds. In 24 scenarios, the proportion of
466 additional newly infected herds that were detected was higher than 0.15 (Figure 9). By construction,
467 the test sensitivity value limits the potential number of additional newly infected herds that can be
468 detected by the model (e.g. with a sensitivity of 0.9, the maximum potential proportion of newly
469 infected herds additionally detected is 0.1). On average, the model captured proportions increased by
470 0.125, 0.076, and 0.034 for sensitivity values of 0.4, 0.7 and 0.9, respectively (Figure 9).

471 Using the NewI cost index, the cut-off value allows systematically for a better detection of newly
472 infected herds compared to test results but is associated with a cost in false positives. Only 3
473 scenarios had a negative cost index, whereby it was able to detect more newly infected herds while
474 having less false positives (Figure 10). For all the other scenarios, the additional detection of newly
475 infected herds was always associated with a positive NewI cost index, i.e. a number of additional
476 false positives for each additional true positive detected (Figure 10). This NewI cost index ranged
477 from - 266 to 1055. On average, the cost index value was 98 meaning that for each additional newly
478 infected herd detected, there were an additional 98 false positive herds compared to test results. NewI
479 cost index was <100 for 73% of the scenarios (116/159) (Figure 10). Extremely high values of the
480 cost index (above 500) were associated with a sensitivity of 0.9 for 5 scenarios (Figure 10). These
481 extreme values were also associated with lower proportions of additionally detected newly infected
482 herds (Figure 11.A)). When the proportion of herds additionally detected was above 0.1, the cost
483 index was <100 except in three (Figure 11.A). All scenarios (43) with a high number of newly
484 infected herds (corresponding to $\tau_1=0.107$) had a NewI cost index below 100 (Figure 10 and Figure
485 11.B).

486 **4.2.4 Comparison of cut-off values**

487 The cut-off values varied substantially between scenarios for both indexes (Figure 12). Use of the
488 Youden index resulted in higher cut-off values (mean cut-off equal 0.14 against 0.05 for cost index)
489 (Figure 12). No association between input parameter values (test characteristics, disease dynamics
490 and risk factors parameters) and selection of a cut-off value was found (supplementary material).

491 **5 Discussion**

492 Our simulation study illustrates the added value of a Bayesian Hidden Markov model, the STOC free
493 model, compared to test results alone to detect infected herds in many different contexts. This model
494 was able to predict herd-level probabilities of infection in about 80% of the investigated scenarios.
495 Situations in which the model did not converge and therefore could not provide estimates of the
496 probabilities of infection were mainly related to low sensitivity values. When it converged, the model
497 detected more infected herds compared to test alone in 152 of the 172 scenarios and detected more
498 newly infected herds in only 65 of 172 scenarios. In these scenarios, the STOC free model sensitivity
499 was higher than the herd-level test sensitivity.

500 Test sensitivity had a great impact on the added value of the STOC free model. Indeed, following a
501 test, the total number of infected and newly infected herds still to be detected (false negatives)
502 increases as test sensitivity decreases. The STOC free model was able to detect an important
503 proportion of these undetected infected herds. On average, the model detected around 25% more
504 infected herds when sensitivity was low (0.4) and around 2% more infected herds when the
505 sensitivity was high (0.9), i.e. around 40% and 20% of the herds still to be detected in our simulations
506 (as assumed for the given levels of sensitivity). The range of herd-level test sensitivities evaluated in
507 this study covers the known range of sensitivities for endemic diseases for which control programmes
508 are in place.

509 An increase in the number of newly infected herds detected by the STOC free model was associated
510 with an increase in the number of false positive herds detected in all but one scenario. We quantified
511 the proportion of additional false positives for each additional newly infected herd detected using a
512 cost index. This cost index increased with high test sensitivity and low prevalence corresponding to
513 small numbers of false test negatives. In five scenarios with a high herd-level test sensitivity, the cost
514 index was substantial (above 500, i.e. 500 false positives for each additional true positive herd
515 detected by the model). This tends to advise against using the STOC free model when test sensitivity
516 is high. On the other hand, the cost index was lower (below 100) with low test sensitivity and high
517 incidence, i.e. when the number of newly infected herds still to be detected was high. For decision
518 support, the level of acceptability in terms of extra false positives would differ according to the
519 consequences in a given control programme, and to the possibilities and resources necessary to
520 confirm a herd status with complementary testing.

521 Different reasons could explain the fact that the STOC free model did not reach convergence in a
522 number of scenarios. In this study, we limited the number of burn-in and sampling iterations to
523 reduce computing time (around 3.5 hours per scenario). For scenarios that did not meet our
524 convergence criterion, re-running the model with more burn-in iterations allowed convergence in
525 around 50% of cases. Adding more iterations could address the remaining convergence issues. A
526 larger population (number of herds) would increase available data (especially in terms of numbers of
527 infected herds) to estimate parameters values. We did not further investigate these hypotheses due to
528 computing time constraint for both simulation and analysis. Low test performance also led to
529 convergence issues. Indeed, as test sensitivity and specificity decrease, the contribution of test results
530 to defining the latent status decreases whereas the contribution of model parameters accounting for
531 new infection and elimination of infection increases. In our study, given the relatively wide prior
532 distributions put on the association between the risk factor and the probability of new infection, this

533 association was estimated from the data. This means that in the scenarios in which test performance
534 was poor, the contribution of surveillance data to estimation and prediction could be expected to be
535 small, which could have made it more difficult for the model to converge. Such estimation issues
536 have already been described in state-space models, when measurement error is high (Auger-Méthé et
537 al., 2016). In such cases, increase the sample size (e.g. the number of herds) or adding prior
538 information could reduce this issue. In our study, informative priors were used for measurement error
539 parameters (sensitivity and specificity) assuming that relevant epidemiological quantities would be
540 known beforehand. To decrease convergence issue, it could be hypothesised that a good knowledge
541 of the strength of association between risk factors and the probability of new infection facilitates
542 convergence by reducing uncertainty around latent statuses. This knowledge would need to be
543 translated into narrow prior distributions.

544 The frequency and strength of the risk factor did not influence the STOC free model performances,
545 contrary to our assumptions. The inclusion of RFs was expected to improve the detection of newly
546 infected herds when they strongly contribute to the risk of new infections (high strength of
547 association). This added value was especially expected to be important when test sensitivity is poor,
548 because knowing that a RF is present could compensate for the lack of sensitivity. In our study, only
549 one RF was included to establish its influence on model performance. More RFs can easily be added
550 to the logistic regression if necessary. The choice of RFs to be included must be based on specific
551 knowledge of infection dynamics within the CP.

552 A cut-off value is needed to classify herds as infected or uninfected from the distributions of
553 probabilities of infection predicted by the STOC free model. The cut-off value varied depending on
554 the method of selection and the simulated context. In the field, the “best” cut-off value would also
555 depend on the objective of the CP. The Youden index equally values sensitivity and specificity
556 without other constraint (i.e. separates at best infected versus non infected herds), while our NewI

557 cost index ensures the detection of a higher number of newly infected herds than the test alone. For
558 most scenarios, the cut-off value identified with the cost index was lower than the cut-off value
559 identified with the Youden index. Indeed, given an endemic situation, the probability of becoming
560 infected is lower than the probability of remaining infected. The specific detection of newly infected
561 herds, that have not been detected by the test, requires a lower cut-off value compared to the cut-off
562 value selected without this constraint. To compute our cost index associated with the detection of a
563 higher number of newly infected herds we gave the same weight to false positives and false
564 negatives. These two types of misclassification have different consequences: in the context of cattle
565 trade, introducing a false negative into a disease free herd is more damaging than not allowing a false
566 positive to be introduced. Whatever the method of selection used, cut-off values were highly variable
567 between the simulated contexts. According to our study, it does not seem possible to determine a cut-
568 off value directly from CP characteristics. However, we can argue that low cut-off values should be
569 favoured where the objective is safe trade, i.e. limiting false negative herds. In real data where no
570 gold standard is available, the choice of the cut-off value has to rely on another method. This point is
571 an important question when this framework is applied to real data and it needs more exploration.

572 Applying the STOC free model to real CPs also requires previous knowledge about the distributions
573 of the model parameters. The choice of prior distributions will be crucial because when the prior
574 distributions deviate too much from the true parameter values, this may lead to convergence issues or
575 bias in the posterior distributions. In this simulation study, true parameter values were known,
576 allowing prior distributions to be centred on the true parameter values. In the context of real CPs, test
577 characteristics are almost always assessed before designing the CP. However, even if information is
578 often available, its interpretation must be made in relation to the targeted latent status which may
579 differ from the definition used in the literature and can be challenging (Duncan et al., 2016). Test
580 characteristics may change depending on the latent status of interest. Information on risk factor of

581 introduction is often available as controlling them is a key measure in CPs to reduce the spread of
582 infection between herds (Lindberg and Houe, 2005). Quantitative data can be derived from the
583 literature (e.g. risk factor study, meta-analysis) but are highly variable between territories and not
584 always available for a specific territory (van Roon et al., 2020a). The model makes it possible to use
585 more or less precise priors according to the available information in the population of interest.

586 Within a CP, the dynamics of the infection (incidence and clearance of infection) as well as the
587 contribution of risk factors are expected to change over time given that the majority of CPs generally
588 act on both preventing new infections and eliminating the pathogen from infected herds. Depending
589 on the CP, these changes may be observed over different periods of time. Example of CPs against
590 BVDV have shown that the decrease in prevalence and incidence in European countries occurred
591 over different time lapses (Houe et al., 2014; Joly et al., 2001; Presi et al., 2011). Risk factor
592 contribution (frequency and strength) may also change during a CP. For example, neighbourhood
593 risk of introduction is linked to infection prevalence in the area. When the prevalence decreases in the
594 territory, the strength of association between having contact with neighbouring herds and becoming
595 infected will decrease, while the frequency of contacts between herds remains the same. In our study,
596 infection dynamics and the contribution of the risk factors remained stable over time to simplify
597 parameter estimations. The changes in infection dynamics and contribution of RFs to new infections
598 could be accommodated by running the model over short time periods (e.g. 1 to 3 years), using the
599 parameter posterior distributions for one period as the prior distributions for the next one.

600 The decrease of infection prevalence and incidence with time during a CP can influence
601 performances of the STOC free model. Here, the cost index was higher when incidence and
602 prevalence were low, reflecting a lower positive predictive value, when the number of true positive
603 herds decreases in a population (similarly to surveillance based on tests only). Therefore, we
604 speculate that the use of the STOC free model will be more interesting with disease present at an

605 endemic level in a population rather than when CP results in decreased prevalence close to
606 eradication.

607 **6 Conclusion**

608 This simulation study demonstrated the capacity of a Hidden Markov Model using disease dynamics
609 and risk factor information from surveillance programmes to detect more infected herds and newly
610 infected herd than test results alone. The added value of the model depends on the context in which a
611 control programme is conducted. It was greatest in situations with low sensitivity tests. However,
612 these situations were also the ones in which the convergence of the model was the most difficult. The
613 added value of the model did not depend on the strength and frequency of the risk factor. The use of
614 the model is likely to be beneficial especially in the early stages of a control programme (when
615 prevalence and incidence are at moderate level) rather than close to eradication.

616 **7 References**

- 617 Auger-Méthé, M., Field, C., Albertsen, C.M., Derocher, A.E., Lewis, M.A., Jonsen, I.D., Flemming,
618 J.M., 2016. State-space models' dirty little secrets: Even simple linear Gaussian models can
619 have estimation problems. *Sci. Rep.* 6, 1–10. <https://doi.org/10.1038/srep26677>
- 620 Cameron, A.R., 2012. The consequences of risk-based surveillance: Developing output-based
621 standards for surveillance to demonstrate freedom from disease. *Prev. Vet. Med.* 105, 280–286.
622 <https://doi.org/10.1016/j.prevetmed.2012.01.009>
- 623 Christensen, J., Gardner, I.A., 2000. Herd-level interpretation of test results for epidemiologic studies
624 of animal diseases. *Prev. Vet. Med.* 45, 83–106. [https://doi.org/10.1016/S0167-5877\(00\)00118-](https://doi.org/10.1016/S0167-5877(00)00118-5)
625 5
- 626 Duncan, A.J., Gunn, G.J., Humphry, R.W., 2016. Difficulties arising from the variety of testing

627 schemes used for bovine viral diarrhoea virus (BVDV). *Vet. Rec.* 178, 292 LP – 292.
628 <https://doi.org/10.1136/vr.103329>

629 Duncan, A.J., Humphry, R.W., 2016. Difficulties arising from the variety of testing schemes used for
630 bovine viral diarrhoea virus. *Vet. Rec.* 178, 292–292. <https://doi.org/10.1136/vr.103329>

631 Gelman, A., Rubin, D.B., 1992. Inference from iterative simulation using multiple sequences. *Stat.*
632 *Sci.* 7, 457–511. <https://doi.org/10.2307/2246134>

633 Houe, H., Nielsen, S.S., Nielsen, L.R., 2014. Control and Eradication of Endemic Infectious diseases
634 in Cattle. London: College Publications.

635 Joly, A., Beaudou, F., Seegers, H., 2001. Evaluation de la prévalence et de la dynamique de
636 l'infection par le virus de la maladie des muqueuses en Bretagne à l'aide d'un test ELISA sur
637 lait de grand mélange. *Epidémiologie Santé Anim.* 7–14.

638 Lindberg, A., Houe, H., 2005. Characteristics in the epidemiology of bovine viral diarrhea virus
639 (BVDV) of relevance to control. *Prev. Vet. Med.* 72, 55–73.
640 <https://doi.org/10.1016/j.prevetmed.2005.07.018>

641 Madouasse, A., Mercat, M., van Roon, A., Graham, D., Guelbenzu, M., Berends, I.S., van Schaik,
642 G., Nielen, M., Frössling, J., Ågren, E., Humphry, R., Eze, J., Gunn, G., Henry, M., Gethmann,
643 J., More, S., Fourichon, C., 2020. A modelling framework for the prediction of the herd-level
644 probability of infection from longitudinal data. *bioRxiv* 1–36.
645 <https://doi.org/10.1101/2020.07.10.197426>

646 Madouasse, A., Mercat, M., Van Roon, A., Graham, D., Guelbenzu, M., Berends, I.S., Van Schaik,
647 G., Nielen, M., Frössling, J., Ågren, E., Humphry, R.W., Eze, J., Gunn, G.J., Henry, M.K.,
648 Gethmann, J., More, S.J., Toft, N., Fourichon, C., 2021. A modelling framework for the

649 prediction of the herd-level probability of infection from longitudinal data. bioRxiv 197426, ve,
650 1–31. <https://doi.org/10.1101/2020.07.10.197426>

651 McAloon, C.G., Doherty, M.L., Whyte, P., Verdugo, C., Toft, N., More, S.J., O’Grady, L., Green,
652 M.J., 2019. Low accuracy of Bayesian latent class analysis for estimation of herd-level true
653 prevalence under certain disease characteristics—An analysis using simulated data. *Prev. Vet.*
654 *Med.* 162, 117–125. <https://doi.org/10.1016/j.prevetmed.2018.11.014>

655 Nielsen, S.S., Toft, N., 2008. Ante mortem diagnosis of paratuberculosis: A review of accuracies of
656 ELISA, interferon- γ assay and faecal culture techniques. *Vet. Microbiol.* 129, 217–235.
657 <https://doi.org/10.1016/j.vetmic.2007.12.011>

658 Plummer, M., 2003. JAGS : A program for analysis of Bayesian graphical models using Gibbs
659 sampling JAGS : Just Another Gibbs Sampler. *Proc 3rd Int Work Distrib Stat Comput (DSC*
660 *2003)*.

661 Presi, P., Struchen, R., Knight-Jones, T., Scholl, S., Heim, D., 2011. Bovine viral diarrhoea (BVD)
662 eradication in Switzerland-Experiences of the first two years. *Prev. Vet. Med.* 99, 112–121.
663 <https://doi.org/10.1016/j.prevetmed.2011.01.012>

664 R Core Team, 2017. R: A language and Computing.

665 Raaperi, K., Orro, T., Viltrop, A., 2014. Epidemiology and control of bovine herpesvirus 1 infection
666 in Europe. *Vet. J.* 201, 249–256. <https://doi.org/10.1016/j.tvjl.2014.05.040>

667 Rangel, S.J., Paré, J., Doré, E., Arango, J.C., Côté, G., Buczinski, S., Labrecque, O., Fairbrother,
668 J.H., Roy, J.P., Wellemans, V., Fecteau, G., 2015. A systematic review of risk factors associated
669 with the introduction of *Mycobacterium avium* spp. paratuberculosis (MAP) into dairy herds.
670 *Can. Vet. J.* 56, 169–177.

671 van Roon, A.M., Mercat, M., van Schaik, G., Nielen, M., Graham, D.A., More, S.J., Guelbenzu-
672 Gonzalo, M., Fourichon, C., Madouasse, A., Santman-Berends, I.M.G.A., 2020a. Quantification
673 of risk factors for bovine viral diarrhoea virus in cattle herds: A systematic search and meta-
674 analysis of observational studies. *J. Dairy Sci.* 103, 9446–9463.
675 <https://doi.org/10.3168/jds.2020-18193>

676 van Roon, A.M., Santman-Berends, I.M.G.A., Graham, D., More, S.J., Nielen, M., van Duijn, L.,
677 Mercat, M., Fourichon, C., Madouasse, A., Gethmann, J., Sauter-Louis, C., Frössling, J.,
678 Lindberg, A., Correia-Gomes, C., Gunn, G.J., Henry, M.K., van Schaik, G., 2020b. A
679 description and qualitative comparison of the elements of heterogeneous bovine viral diarrhoea
680 control programs that influence confidence of freedom. *J. Dairy Sci.* 103, 4654–4671.
681 <https://doi.org/10.3168/jds.2019-16915>

682 Whittington, R., Donat, K., Weber, M.F., Kelton, D., Nielsen, S.S., Eisenberg, S., Arrigoni, N., Juste,
683 R., Sáez, J.L., Dhand, N., Santi, A., Michel, A., Barkema, H., Kralik, P., Kostoulas, P., Citer, L.,
684 Griffin, F., Barwell, R., Moreira, M.A.S., Slana, I., Koehler, H., Singh, S.V., Yoo, H.S.,
685 Chávez-Gris, G., Goodridge, A., Ocepek, M., Garrido, J., Stevenson, K., Collins, M., Alonso,
686 B., Cirone, K., Paolicchi, F., Gavey, L., Rahman, M.T., De Marchin, E., Van Praet, W.,
687 Bauman, C., Fecteau, G., McKenna, S., Salgado, M., Fernández-Silva, J., Dziejzinska, R.,
688 Echeverría, G., Seppänen, J., Thibault, V., Fridriksdottir, V., Derakhshandeh, A., Haghkah, M.,
689 Ruocco, L., Kawaji, S., Momotani, E., Heuer, C., Norton, S., Cadmus, S., Agdestein, A.,
690 Kampen, A., Sztejn, J., Frössling, J., Schwan, E., Caldow, G., Strain, S., Carter, M., Wells, S.,
691 Munyeme, M., Wolf, R., Gurung, R., Verdugo, C., Fourichon, C., Yamamoto, T., Thapaliya, S.,
692 Di Labio, E., Ekgatit, M., Gil, A., Alesandre, A.N., Piaggio, J., Suanes, A., De Waard, J.H.,
693 2019. Control of paratuberculosis: Who, why and how. A review of 48 countries. *BMC Vet.*
694 *Res.* 15, 1–29. <https://doi.org/10.1186/s12917-019-1943-4>

695 Youden, W.J., 1950. Index for rating diagnostic tests. *Cancer* 3, 32–35. <https://doi.org/10.1002/1097->
696 0142(1950)3:1<32::AID-CNCR2820030106>3.0.CO;2-3

697

698

699 Table 1: Parameter values for scenario simulation.

Parameter	Description	Value	Condition ¹
$nherds$	Number of herds	5000	-
$nTests$	Number of test times per herd	6	-
Se	Herd-level sensitivity	0.4, 0.7, 0.9	-
Sp	Herd-level specificity	0.8, 0.95	-
P	Prevalence of infection	0.1, 0.3	-
τ_2	Probability of remaining infected	0.75, 0.9	-
τ_1	Probability of becoming infected	0.011, 0.028, 0.043, 0.107	Depends on τ_2 and P values
γ	Relative risk associated with X	1.5, 2, 5	-
F	Frequency of X	0.1, 0.25, 0.5	-
β	Probability of new infection for an uninfected herd without X	0.004, 0.005, 0.007, 0.008, 0.009, 0.010, 0.014, 0.019, 0.020, 0.021, 0.022, 0.025, 0.027, 0.029, 0.031, 0.034, 0.036, 0.038, 0.039, 0.041, 0.054, 0.071, 0.076, 0.086, 0.086, 0.095, 0.097, 0.102	Depends on τ_1 , γ and F value

700 ¹ The condition column details the dependencies between parameters, for parameters whose values
 701 are derived from the combination of values of other parameters.

702 Table 2: Prior distribution for the model parameters.

Parameter	Description	Distribution	Mean	Variance
\widehat{Se}	Herd-level test sensitivity	<i>Beta</i>	True value	0.0025
\widehat{Sp}	Herd-level test specificity	<i>Beta</i>	True value	0.0025
$\widehat{\tau}_2$	Probability for an infected herd not to eliminate the infection	<i>Beta</i>	True value	0.0025
$\widehat{\theta}_1$	Intercept (risk factor)	<i>Normal</i>	True value	1
$\widehat{\theta}_2$	Coefficient (risk factor)	<i>Normal</i>	True value	1
$\widehat{\pi}_{i,1}$	Probability of being infected at time 1	<i>Beta</i>	Prevalence true value	0.0225

703

704

705

706 Table 3: Number of scenarios that converged depending on each value of the simulated parameters.

Parameter	Value	Initial number of scenarios	Number of scenarios that converged
Se	0.4	72	34
	0.7	72	66
	0.9	72	72
Sp	0.8	108	74
	0.95	108	98
P	0.1	108	91
	0.3	108	81
τ_1	0.0111	54	45
	0.0278	54	46
	0.0429	54	38
	0.1071	54	43
τ_2	0.75	108	89
	0.9	108	83
F	0.1	72	62
	0.25	72	57
	0.5	72	53
γ	1.5	72	61
	2	72	59
	5	72	52

707

708

709

710

711

712

713

714

Figure captions

Figure 1: Representation of the design strategy. Variables in rectangles represent observational data (risk factor and test results). Variables in circles represent herd infection statuses: true simulated status in solid line and latent estimated/predicted status in dashed line. Observational data simulated using the simulation model are used as input for the STOC free model. Herd statuses predicted by the STOC free model on the 6th time-step are compared to the corresponding simulated statuses, considered as the gold standard.

Figure 2: Representation of the STOC free model prediction performance analysis. At first stage posterior herd probability of being infected are summarized using the median value. Then, categorization of herds is done by applying a cut-off to the distribution of posterior median. Cut-off determination is based on two different indexes. Finally, the performance of the STOC free model is obtained by comparing the number of true positives using the STOC free model and the number of true positives obtained using test information alone.

Figure 3: Proportion of scenarios that converged for each simulation parameter value. Six of the seven simulated parameters are represented : Se (test sensitivity), Sp (test specificity), P (prevalence), τ_2 (probability of remaining infected), F (frequency of the risk factor) and γ (relative risk associated with the risk factor).

Figure 4 : Proportion of scenarios that converged for all combinations of Se (test sensitivity) and Sp (test specificity) values.

Figure 5: Difference between the number of herds accurately classified by the STOC free model and the number of herds accurately classified using test results for infected herds only, for uninfected herds and for all herds. Dark blue diamond represents the mean of each

distribution. At the dashed grey line, the STOC free model and test results accurately classified the same numbers of herds.

Figure 6: Additional proportion of infected herds accurately classified by the STOC free model relative to test results, among the total number of infected herds, depending on simulated parameter values, using cut-off found applying Youden index. The seven simulated parameters are represented : Se (test sensitivity), Sp (test specificity), F (frequency of the risk factor), γ (relative risk associated with the risk factor), P (prevalence), τ_1 (probability of being newly infected) and τ_2 (probability of remaining infected). Dark blue diamond represents the mean of each distribution. At the dashed grey line, the STOC free model and test results accurately classified the same numbers of herds.

Figure 7: Difference between the number of herds accurately classified by the STOC free model and the number of herds accurately classified using test results only for herds which were candidates for new infection at the final time-step (i.e. herds that were uninfected at the previous step time) for newly infected herds, uninfected herds and all herds, using cut-off found applying Youden index. Dark blue diamond represents the mean of each distribution. At the dashed grey line, the STOC free model and test results accurately classified the same numbers of herds.

Figure 8: Additional proportion of newly infected herds detected by the STOC free model relative to test results, among the total number of newly infected herds, depending on simulated parameter values, using cut-off found applying Youden index. The seven simulated parameters are represented : Se (test sensitivity), Sp (test specificity), F (frequency of the risk factor), γ (relative risk associated with the risk factor), P (prevalence), τ_1 (probability of being newly infected) and τ_2 (probability of remaining infected). Dark blue diamond

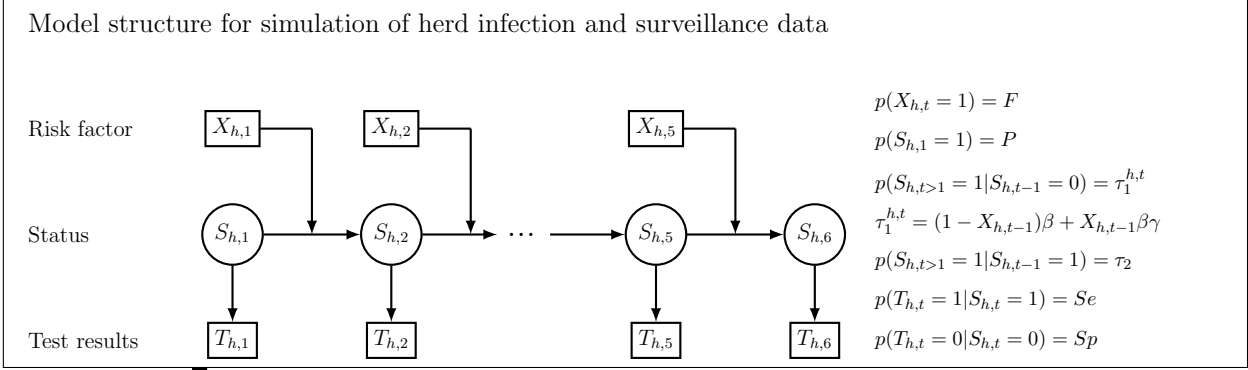
represents the mean of each distribution. At the dashed grey line, the STOC free model and test results accurately classified the same numbers of herds.

Figure 9: Additional proportion of newly infected herds detected by STOC free model relative to test results, among the total number of newly infected herds, depending on simulated parameter values, using cut-off found applying NewI cost index. The seven simulated parameters are represented : Se (test sensitivity), Sp (test specificity), F (frequency of the risk factor), γ (relative risk associated with the risk factor), P (prevalence), τ_1 (probability of being newly infected) and τ_2 (probability of remaining infected). Dark blue diamond represents the mean of distribution. At the dashed grey line, the STOC free model and test results accurately classified the same numbers of herds.

Figure 10: Cost index value, i.e. the number of additional false positive herds for each additional true positive herds by the STOC free model relative to test results, depending on simulated parameter values, using cut-off found applying NewI cost index. The seven simulated parameters are represented : Se (test sensitivity), Sp (test specificity), F (frequency of the risk factor), γ (relative risk associated with the risk factor), P (prevalence), τ_1 (probability of being newly infected) and τ_2 (probability of remaining infected). Dark blue diamond represents the mean of distribution. Under the dashed grey line cost is negative meaning that STOC free model do detect more newly infected for less false positive herds compared to test results.

Figure 11: Cost index value, i.e. the ratio of additional false positive herds on the additional true positive herds, using cut-off found applying NewI cost index, depending on the proportion of additional newly infected herds detected (A) and the number of newly infected herds which depend on the four possible values of the probability of become infected (τ_1).

Figure 12: Distribution of cut-off values for herd status classification depending on the index used. “NewI” criterion is based on a trade-off between the additional number of true positive herds and the additional number of false positive herds. “Youden” criterion is based on maximizing sensitivity and specificity based on classification of all herds. Dark blue diamond represents the mean of the distribution.

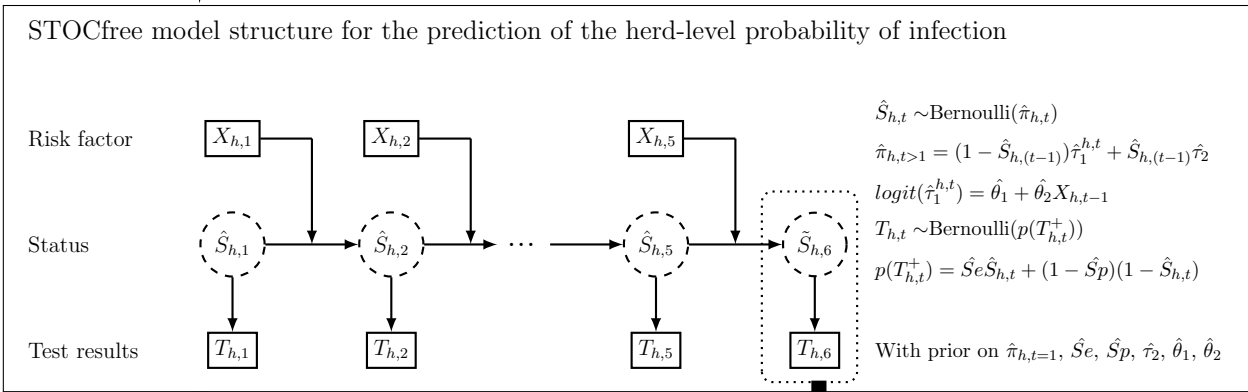


Parameters that vary among simulated scenarios

Infectious dynamics parameters: P , τ_2 and τ_1

Risk factor effect parameters: F , γ and β

Tests performances parameters: Se and Sp



Evaluation of model parameter estimation
 $\hat{Se}, \hat{Sp}, \hat{\tau}_2, \hat{\theta}_1, \hat{\theta}_2$

Markov Chain

Assessing MCMC convergence
Gelman-rubin statistics

Posterior distribution

Assessing parameter estimation accuracy
Posterior distribution vs simulated population value

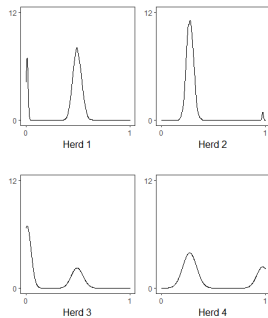
Evaluation of model prediction

Posterior herd level probability of being infected $p(\tilde{S}_{h,6})$

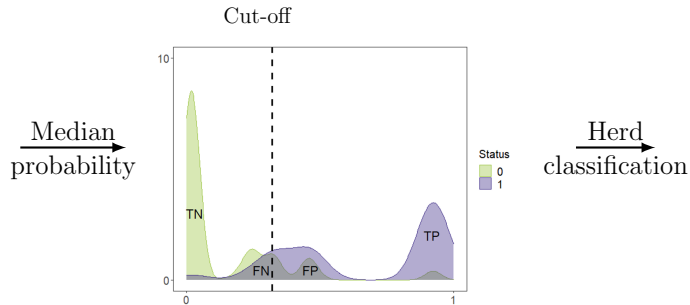
Assessing prediction performances
Comparison of (newly) infected herds detected by :

- the test
- the STOCfree model

Herd level posterior probability of being infected



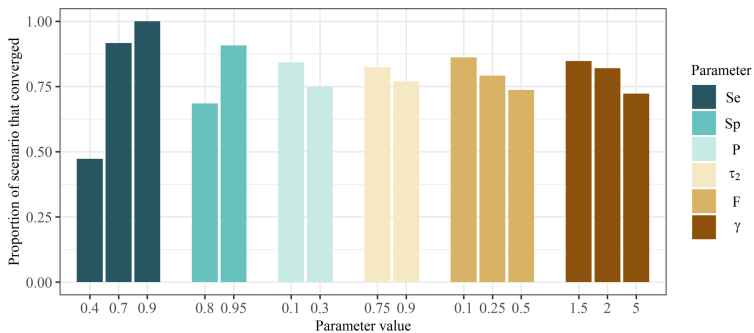
Distribution of median probability of being infected



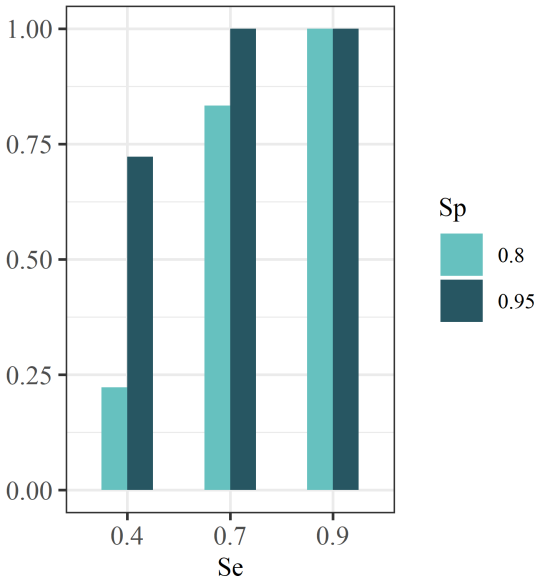
STOC free model performances

Proportion of infected herds additionally detected compared to test:

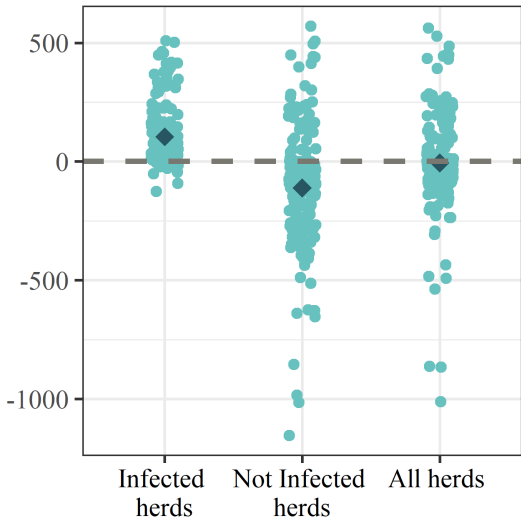
$$\frac{TP_{STOC\ free} - TP_{test}}{\text{Number of infected herds}}$$



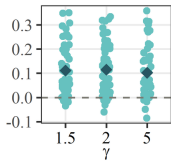
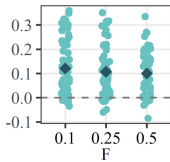
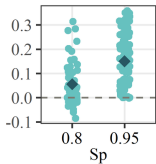
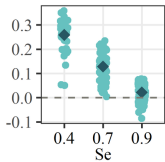
Proportion of scenario that converged



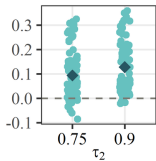
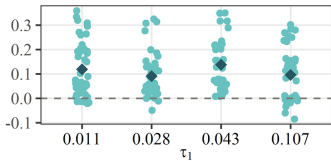
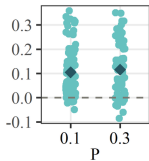
Number of additional herds accurately classified



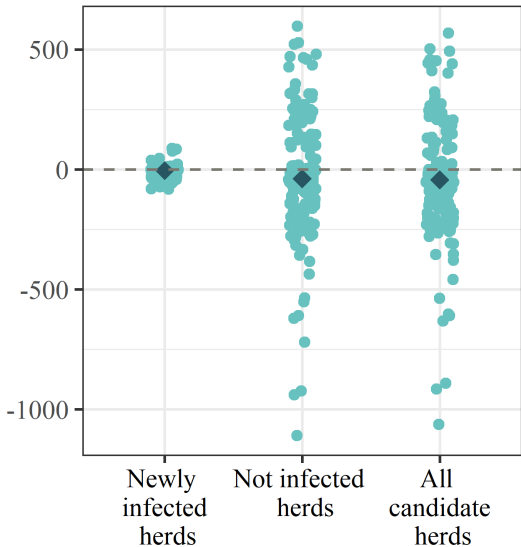
Additional proportion of
infected herds detected

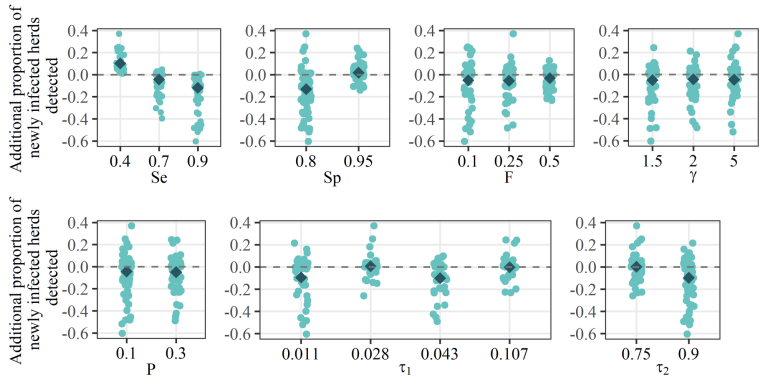


Additional proportion of
infected herds detected

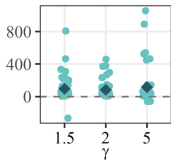
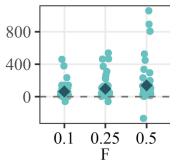
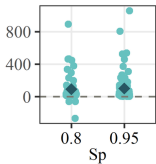
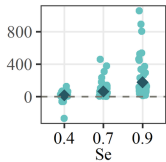


Number of additional herds candidate
to new infection accurately classified





Cost index



Cost index

